ELSEVIER

FTIR investigation of CTAB–Al–montmorillonite complexes

Weihong Xue [a,b], Hongping He [a,*], Jianxi Zhu [a], Peng Yuan [a]

[a] *Guangzhou Institute of Geochemistry, Chinese Academy of Sciences, Guangzhou 510640, China*
[b] *Graduate School of Chinese Academy of Sciences, Beijing 100039, China*

Abstract

In this study, CTAB–Al–montmorillonite complexes were synthesized by pre-modifying montmorillonite using different concentrations of surfactant (resulting in different surfactant loadings and basal spacings), then pillaring the organoclays with hydroxy-Al cations. The resultant inorganic–organic montmorillonite complexes were characterized using FTIR, with a combination of XRD, TG and chemical analysis. This study indicates that the basal spacings of the CTAB–Al–montmorillonite complexes and the amounts of Al-contained pillars strongly depend on the surfactant loadings in the clay interlayer space, resulted from the mobility variation of the intercalated surfactants. During pillaring hydroxy-Al cations into clay interlayer space, part of the intercalated surfactants were removed, resulting in a decrease of the ordering of alkyl chains and the frequency shifts of Si(Al)–O, Si–O–Al and (M–O)$_{Td}$ stretching vibrations. The hydrophobicity of the CTAB–Al–montmorillonite complex also strongly depends on the surfactant loading whereas that of the CTAB–Al–montmorillonite complex is relative lower than that of the corresponding organoclay, indicated by the frequency shift of the vibrations corresponding to the sorbed water and their contents estimated by TG curves. With the decrease of the sorbed water content, the frequency of the band of H–O–H bending (v_2) shifts to higher frequency while the O–H stretching vibration (v_1 and v_3) shifts to lower frequency, indicating that H$_2$O is less hydrogen bonded. Meanwhile, the ordered conformations of the alkyl chains in CTAB–Al–montmorillonite complex decrease when compared with that of the corresponding organoclay.
© 2006 Elsevier B.V. All rights reserved.

Keywords: FTIR spectrum; Sorbed water; Surfactant; Hydroxy-Al cations; CTAB–Al–montmorillonite complexes

1. Introduction

Montmorillonite is a kind of 2:1 type layered silicates. Because of an isomorphic substitution within the layers (for example, Al^{3+} replaced by Mg^{2+} or Fe^{2+}, or Mg^{2+} replaced by Li$^+$ in the octahedral sheet, Si^{4+} replaced by Al^{3+} in the tetrahedral sheet), the clay layer is negatively charged, which is counterbalanced by cations in the interlayer space. These cations are exchangeable and the sum of their charges is the cation exchange capacity (CEC).

In past decades, pillared interlayer clays (PILCs) and organoclays have attracted extensive attention due to the important applications in a variety of fields [1–3]. PILCs have been widely used as catalyst carriers and catalysts while organoclays are used to prepare clay-based nanocomposites and as sorbents to remove organic pollutants [3]. Both of PILCs and organoclays are prepared by replacing the exchangeable interlayer cations

with metal hydrolysates and surfactants, respectively [3]. The CEC value of the used clay determines the number of metal hydrolysates and cationic surfactants that can be intercalated into the clay interlayer space [4]. In the case of PILCs, the specific surface area and pore volume are greatly improved [5], which are important when they are used as catalysts and sorbents. Due to the hydrophilic surfaces of PILCs, they show poor affinity to organic pollutants. However, after modified with surfactants, the resultant organoclays show high efficiency to remove organic pollutants in water [6,7]. Here, an interesting idea comes out that the materials may show excellent sorption efficiency to organic pollutants if clays are pillared/modified by both metal hydrolysates and surfactants. This assumption is on the basis of the facts that pillaring clays with metal hydrolysates results in a prominent improvement of clay interlayer space (including specific surface area and pore volume) and modifying clays with surfactants leads to the transformation of hydrophilic clay surfaces to hydrophobic ones [8]. Hence, inorganic–organic clay complexes might be of great potential applications in remediation of polluted environments. Recently, great efforts have been paid on synthesis and application of inorganic–organic clay

---

complexes [8–11]. Wu et al. [9] found that modifying inorganic-pillared montmorillonites with surfactant could greatly improve their sorbing capacity to phenol. By preadsorption of organic molecules (amines) between the clay layers prior to pillaring with aluminium precursor, it was possible to increase the microporosity of the obtained materials [11]. However, up to now, there are few studies on the interlayer structure and surface properties of the inorganic–organic clay complexes, which are of high importance for the synthesis and applications.

In the previous studies, the inorganic–organic clay complexes were prepared by the route of pillaring clays with metal hydrolysates, followed by modifying the pillared clays with surfactants. In this case, the interlayer space strongly depends on the inorganic pillars. In this study, the inorganic–organic clay complexes were prepared by pre-modifying clays with different concentrations of surfactant (cetyltrimethyl ammonium bromide, CTAB), then pillaring the organoclays with hydroxy-Al cations (the resulted materials were denoted as CTAB–Al–Mt complexes). The resultant inorganic–organic clay complexes were characterized using FTIR, with a combination of XRD, TG and chemical analysis.

FTIR is a useful way to investigate the characteristics of clays and the related materials [12–16]. For example, the frequencies of the asymmetric and symmetric CH_2 stretching absorption bands are sensitive to the conformation of the intercalated surfactants within the clay interlayer space [16]. The change of the clay surface affinity (hydrophobic and hydrophilic) can be indicated by the frequency shifts and intensity of hydroxyl stretching and bending vibrations of the sorbed water [16]. The changes of the Al–OH vibration bands can also reflect the interaction between hydroxy-Al cations and clay layers [12,13].

The aim of this study is to investigate the microstructure of CTAB–Al–Mt complexes and the effect resulted from the pre-modified surfactant loadings. This study provides some new insights in the synthesis of inorganic–organic clay complexes and the interlayer structure of the resulting materials. It is important for well understanding the structure and properties of inorganic–organic clays and their applications.

2. Experimental

2.1. Synthesis of CTAB–Al–Mt complexes

The montmorillonite (Ca–Mt) was supplied by Nanhai Mining Ltd., China. The sample was purified by sedimentation and the <5 μm size fraction was collected and dried at 80 °C. The sample was grounded through 200 meshes and sealed in a glass tube for use. The structural formula of Ca–Mt can be expressed as $(Na_{0.009}Ca_{0.193}Mg_{0.064})(Fe_{0.086}Mg_{0.475}Al_{1.440})(Si_{3.96}Al_{0.04})$ $O_{10}(OH)_{10} \cdot nH_2O$, deduced from the chemical analysis result. Its cation exchange capacity (CEC) is 64.8 mmol/100 g, determined by NH_4^+ method as described in the literature [17]. The reagents used in this study were of analytical grade.

The synthesis of CTAB–Al–Mt complexes contains three basic steps. Firstly, Na–montmorillonite (Na–Mt) was prepared from Ca–Mt, following the method reported in our previous study [18]. Then, organoclays were prepared using Na–Mt and CTAB under different CTAB concentrations as described in the literature [18]. The organoclay prepared at the CTAB concentration of 0.2 CEC is denoted as 0.2CTAB–Mt and the others are marked in the same way. The resultant organoclays were dried at 80 °C, grounded through 200 meshes and kept in a sealed bottle. Secondly, the pillaring solution was prepared from 0.2 M of $AlCl_3 \cdot H_2O$ solution and 0.2 M of Na_2CO_3 solution with a ratio of OH/Al = 2.4. The sodium carbonate solution was incorporated drop by drop into the aluminium chloride solution. This oligomeric solution was allowed to age for 24 h at 80 °C under constant agitation on a stir plate. Finally, CTAB–Al–Mt complexes were synthesized by intercalation of hydroxy-Al cations into organoclays. The organoclays (4.5 g) were dispersed in 1 L of deionized water and the Al-pillaring solution was incorporated drop by drop into the slurry containing the organoclays with a ratio of Al/clay = 10 mmol g^{-1}. The pH of this mixture was adjusted to 3.9 and the mixture was stirred for 12 h. The resultant material was centrifuged and washed with deionized water until no chloride present in the decanted water (tested with $AgNO_3$). The resultant material was then dried overnight at 80 °C in a conventional drying oven. The products were denominated as 0.2CTAB–Al–Mt, 0.7CTAB–Al–Mt, 2.0CTAB–Al–Mt and 3.0CTAB–Al–Mt, respectively, corresponding to the used organoclays. For comparison, one sample of Na–Mt pillared with hydroxy-Al cations was prepared using the same ratio of Al/clay = 10 mmol g^{-1} (marked as Al–Mt).

2.2. Characterization

X-ray diffraction (XRD) patterns were recorded between 1.5° and 18° (2θ) at a scanning speed of 3° min^{-1} using Rigaku D/max-1200 diffractometer with Cu Kα radiation. All samples were analyzed as oriented clay-aggregate specimens prepared by drying the suspensions on glass slides. The chemical compositions of samples were analyzed by wet chemistry method. Thermogravimetric (TG) analysis was carried out on Netzsch STA 449 thermobalance from 25 to 900 °C at a heating rate of 10 °C min^{-1} under nitrogen. Fourier transform infrared spectra (FTIR) using KBr pressed disk technique were gained on Nicolet Nexus 470 Fourier transform infrared spectrometer. For each sample, 0.9 mg sample and 80 mg KBr were weighted and grounded in an agate mortar for 10 min before making the pellets. The spectra were collected for each measurement over the spectral range of 400–4000 cm^{-1} with a resolution of 1 cm^{-1}.

3. Results and discussion

3.1. XRD patterns

The changes of basal spacings of the resulted materials can reflect the intercalations of CTAB and hydroxy-Al cations into montmorillonite interlayer spaces.

Fig. 1 shows the XRD patterns of montmorillonites, Al–Mt, organoclays and CTAB–Al–Mt complexes. For Al–Mt, the d_{001} value is 19.4 Å which is larger than that of Na–Mt (12.4 Å) and agrees well with those of Al-pillared montmorillonites reported in the literatures [19,20], indicating that hydroxy-Al cations
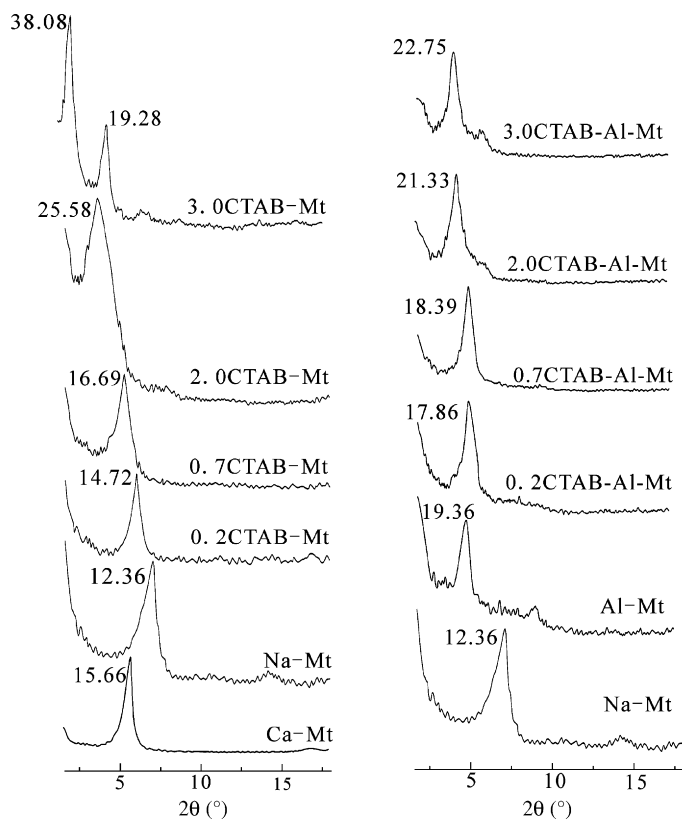
Fig. 1. X-ray diffraction patterns of Ca–Mt, Na–Mt, Al–Mt, organoclays and CTAB–Al–Mt complexes.

Table 1
Main chemical compositions (wt.%) of the samples and the related ratios

Samples	SiO$_2$	Al$_2$O$_3$	Al/Si	Water	Surfactant	C/Si
Na–Mt	64.87	11.92	0.21	6.33	0	0
Al–Mt	54.72	23.87	0.50	8.95	0	0
0.2CTAB–Mt	63.71	11.28	0.20	5.70	4.64	0.13
0.7CTAB–Mt	59.55	11.17	0.21	2.79	12.65	0.36
2.0CTAB–Mt	50.09	10.32	0.23	2.30	28.19	0.97
3.0CTAB–Mt	44.79	8.49	0.22	2.28	34.50	1.33
0.2CTAB–Al–Mt	59.71	19.66	0.37	6.81	4.01	0.12
0.7CTAB–Al–Mt	55.50	18.76	0.38	4.49	8.95	0.28
2.0CTAB–Al–Mt	56.99	13.47	0.27	2.84	17.75	0.54
3.0CTAB–Al–Mt	55.28	12.38	0.25	2.45	22.17	0.69

studies [16,23] demonstrate that surfactant molecules within organoclays with a low loading are separated and show high mobility whereas they are well confined within the clay inter-layer space of the organoclays with high packing density. This can well explain the variation of Al contents in the complexes derived from the organoclays with different surfactant loadings. That is to say, in the case of high surfactant loadings, the sur-factant with a high packing density will hinder the entering of hydroxy-Al cations whereas the hydroxy-Al cations are rela-tively easy to enter into the clay interlayer space in the case of organoclays with low surfactant loadings.

As shown in Table 1, it can also be found that the C/Si ratio of the complex decreases when compared with that of the corresponding organoclay, indicating that some intercalated sur-factants are removed when hydroxy-Al cations enter into the clay interlayer space. This implies that there is an ion exchange between the intercalated surfactant cations and the hydroxy-Al cations.

have been intercalated into montmorillonite interlayer spaces. The XRD patterns of the organoclays are similar to our previous results [18]. With an increase of surfactant concentration in the preparation solution, the basal spacing of the resultant organ-oclays increases in the following order: 12.4 Å (Na–Mt) → 14.7 Å (0.2CTAB–Mt) → 16.7 Å (0.7CTAB–Mt) → 25.6 Å (2.0CTAB–Mt) → 38.1 Å (3.0CTAB–Mt), corresponding to lateral-monolayer, lateral-bilayer, paraffin-monolayer and paraffin-bilayer, respectively [18].

Compared with the corresponding organoclays, a signif-icant change of the basal spacings and aluminium contents in CTAB–Al–Mt complexes can be observed after the corre-sponding organoclays were pillared with hydroxy-aluminium cations. 0.2CTAB–Al–Mt, 0.7CTAB–Al–Mt, 2.0CTAB–Al–Mt and 3.0CTAB–Al–Mt display their basal spacings at 17.86, 18.39, 21.33 and 22.75 Å, respectively, as shown in Fig. 1. Here, it can be found that 0.2CTAB–Al–Mt and 0.7CTAB–Al–Mt display bigger basal spacings than those of the corresponding organoclays whereas 2.0CTAB–Al–Mt and 3.0CTAB–Al–Mt show smaller basal spacings than those of the corresponding organoclays. This implies that the basal spacings of the resul-tant complexes strongly depend on the surfactant loadings within the organoclays.

The contents of Al and Al/Si ratios in Na–Mt, Al–Mt, organ-oclays and the corresponding complexes are shown in Table 1. It can be found that the Al$_2$O$_3$ content in the complex decreases with the increase of the surfactant loading in the corresponding organoclay. Both molecular modeling [21,22] and spectroscopic

3.2. Characteristic vibrations of water

Water molecules exhibit three fundamental vibration modes, i.e. asymmetric stretching vibration (ν_3), symmetric stretch-ing vibration (ν_1) and H–O–H bending vibration (ν_2) [24]. Fig. 2 shows the variation of the absorption band related to the ν_2(H–O–H) bending vibration of water molecules sorbed on montmorillonite and the resulted materials. The band center of Al–Mt locates at ca. 1628 cm^{-1} with a higher intensity com-pared with that of Na–Mt (at ca. 1633 cm^{-1}). This should be attributed to an increase of water content in Al–Mt, resulted from the intercalation of hydroxy-Al cations into the clay interlayer space [25,26]. CTAB–Al–Mt complexes display a broad vibration with a relative lower intensity and the fre-quency shifts from 1630 cm^{-1} (0.2CTAB–Al–Mt) to 1637 cm^{-1} (3.0CTAB–Al–Mt). The frequency shift trend of CTAB–Al–Mt complex is similar to that of organoclay reported in our previ-ous study [16], indicating that the hydrophobicity of the resultant materials increases with the increase of surfactant loading. How-ever, the frequencies of the CTAB–Al–Mt complexes are lower than those of the corresponding organoclays [16]. For example, the ν_2(H–O–H) bending vibration of 3.0CTAB–Al–Mt locates at 1637 cm^{-1} whereas that of the corresponding organoclay (3.0CTAB–Mt) is at 1647 cm^{-1} [16]. This suggests that the
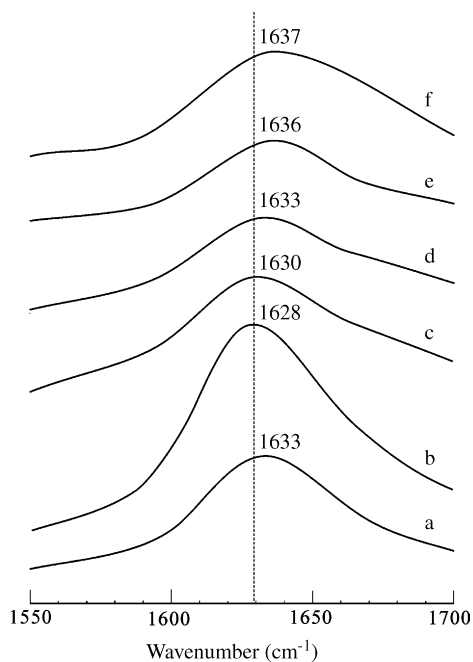
Fig. 2. FTIR spectra of the H–O–H bending region of H_2O: (a) Na–Mt; (b) Al–Mt; (c) 0.2CTAB–Al–Mt; (d) 0.7CTAB–Al–Mt; (e) 2.0CTAB–Al–Mt; (f) 3.0CTAB–Al–Mt.

Fig. 3. FTIR spectra of the O–H stretching region of H_2O: (a) Na–Mt; (b): Al–Mt; (c) 0.2CTAB–Al–Mt; (d) 0.7CTAB–Al–Mt; (e) 2.0CTAB–Al–Mt; (f) 3.0CTAB–Al–Mt.

decrease of the hydrophobicity of the complex results from the inserting of hydroxy-Al cations and removal of some intercalated surfactant.

FTIR spectra of all samples display a band at ca. $3620 \, cm^{-1}$ due to the O–H stretching vibration of the structural O–H groups, and this band is independent on the cation types within clay interlayer space and their contents. This suggests that cation exchange of the interlayer cations has little effect on the structural OH in Al–O(OH) octahedral. The asymmetric vibration (v_3) of H-bonded water cannot be found because the position of the O–H stretching bands cannot be determined unambiguously in this study due to overlapping and broadening of the OH stretching bands [12].

The absorption band at ca. $3450 \, cm^{-1}$, corresponding to the symmetric v_1(O–H) stretching vibration of H-bonded water [27], can be observed for all the studied samples (Fig. 3). Also, it can be seen that its intensity is dependent on the type and the concentration of the interlayer cations. For Al–Mt, the band locates at ca. $3446 \, cm^{-1}$ and the intensity is higher than that of Na–Mt ($3444 \, cm^{-1}$). The former is ascribed to the O–H stretching vibration in hydroxy-Al cations while the latter corresponds to the hydroxyl groups involved in water–water hydrogen bands [20].

For CTAB–Al–Mt complexes, the v_1 mode shifts to lower frequency with the increase of the loaded surfactant. This is caused by the decrease of hydrogen bonding strength in organo-montmorillintes [16]. With the intercalation of surfactants, H_2O content is reduced with the replacement of the hydrated cations by surfactant and the surface of montmorillonite is changed from hydrophilic to hydrophobic. TG analysis provides a supporting evidence for this point. As shown in Table 1, with the increase of the loaded surfactant in montmorillonite, the
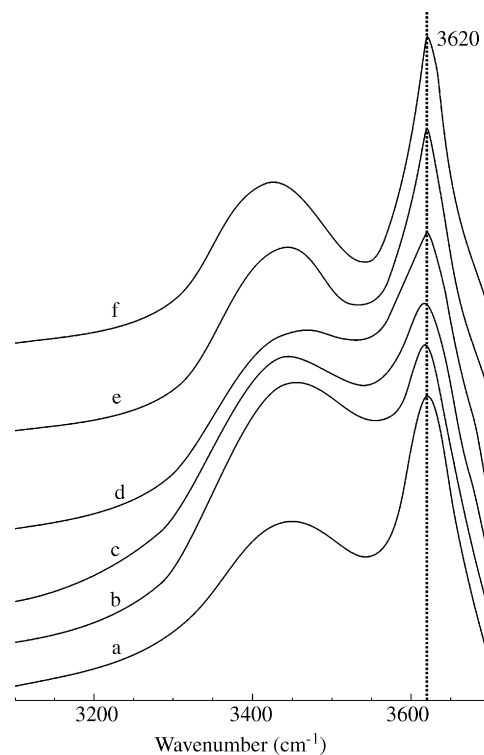
percentage of sorbed water decreases from 8.95% (Al–Mt), 6.81% (0.2CTAB–Al–Mt), 4.49% (0.7CTAB–Al–Mt), 2.84% (2.0CTAB–Al–Mt), to 2.45% (3.0CTAB–Al–Mt). Hence, the surface property change of the resultant complexes leads to a decrease the hydrogen bonding, resulting in a lower frequency shift at v_1(H–O–H) stretching vibration.

Based on the above discussions, it can be concluded that the frequency shift of the H–O–H bending mode (v_2) and O–H stretching modes (v_1 and v_3) of water molecules sorbed on montmorillonite are indicative of the clay surface property.

Previous studies show that, for montmorillonites pillared with hydroxy-Al cations, there is a frequency decrease of the v_2 mode, accompanied by a frequency increase of v_1 and v_3 modes [11,23]. For organoclays, there are a frequency increase of v_2 and a decrease of v_1 and v_3 modes [15]. Our present study is a combination of the above mentioned cases and can be well explained using the conclusions reported in the literatures [12,16,24,7].

The hydrophilic cations will strengthen the H-bonding of the polarized water, so the frequency of v_2 mode decreases and those of v_1 and v_3 modes increase. Yan et al. [28,29] attributed the frequency decrease of v_2 mode to a coupling between H_2O molecules and the Si–O stretching vibrations of the 2:1 layer through the formation of hydrogen bonds. However, the hydrophobic cations will weaken the H-bonding of the polarized water, so the frequency of H–O–H bending vibration (v_2) increases and those of v_1 and v_3 vibrations decrease. For the stronger H-bond, lower energy is required for an occurrence of OH-stretching vibration (v_1 and v_3) and thus a higher frequency of the OH-stretching band can be observed. However, in

this case, more energy is required for H–O–H bending vibration (ν_2) and thus a lower frequency of the H–O–H bending band can be observed [30]. This means that an increase of hydrophobicity of the clay surface will lead to the H–O–H bending vibration shifting to higher frequency and the O–H stretching vibration to lower frequency, and vice versa. In this study, both hydroxy-Al (hydrophilic) and surfactant cations (mainly hydrophobic) are inserted into the clay interlayer space, and the hydrophobicity of the resultant complexes increases with an increase of the loaded surfactant. Hence, the frequency of H–O–H bending vibration (ν_2) increases and those of ν_1 and ν_3 vibrations decrease, but the frequency shifts are less than those for the corresponding organoclays as shown in our previous study [15].

3.3. Surfactant and hydroxy-Al cations in the interlayer space

Previous studies [16,23,31,32] indicated that the ordered conformation of the alkyl chains in the confined system showed a strong dependence on amine concentration and orientation. In relatively high concentration range, the confined amine chains adopt an essentially all-*trans* conformation and the frequency of the asymmetric CH$_2$ stretching absorption band locates at a relatively low frequency. However, in the relatively low amine concentration range, the frequency shifts significantly to higher frequency and the confined amine chains adopt a large number of gauche conformations.

Fig. 4 shows the FTIR spectra of the samples between 2750 and 3050 cm^{-1}. All CTAB–Al–Mt complexes display characteristic vibrations at ca. 2921–2927 and 2851–2853 cm^{-1}, respectively. These two vibrations correspond to the asymmetric and symmetric CH$_2$ stretching modes of amine. It can be seen that the intensities of the vibrations strongly depend on the increase of the loaded surfactant. Comparing the
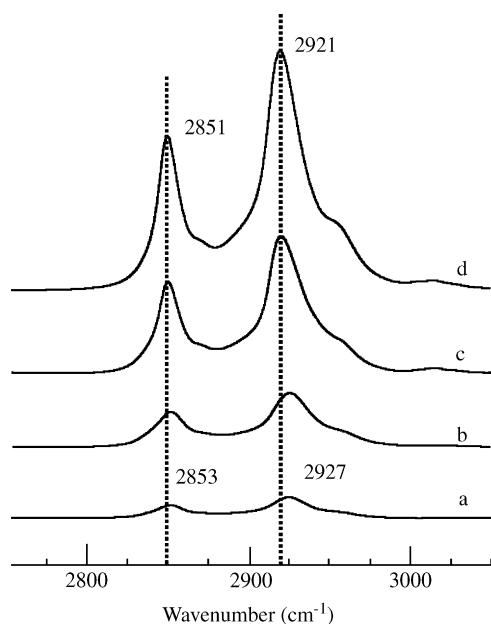
frequencies of CTAB–Al–Mt complexes with those of the corresponding organoclays, it can be found that both vibrations of CTAB–Al–Mt complexes prepared from the organoclays with high surfactant packing density significantly shift to higher frequencies. For example, 3.0CTAB–Al–Mt displays two bands at 2921 cm^{-1} for asymmetric CH$_2$ stretching mode and 2851 cm^{-1} for symmetric CH$_2$ stretching mode. The frequencies are obviously higher than those of the corresponding organoclay (2917 and 2849 cm^{-1}, respectively) and similar to those of the organoclay prepared at about 1.0 CEC [15]. This implies that some intercalated surfactant are removed during the pillaring with hydroxy-Al cations, in accordance with the conclusion made from XRD patterns. This conclusion is further supported by the calculation of C/Si ratios for the CTAB–Al–Mt complexes as shown in Table 1. Our calculation shows that there is a prominent decrease of C/Si ratio for CTAB–Al–Mt complexes than that of the corresponding organoclays.

Fig. 5 shows the FTIR spectra of Na–Mt, Al–Mt and CTAB–Al–Mt complexes in the range of 400–1200 cm^{-1} and the assignments of the vibrations are summarized in Table 2. From Al–Mt to 3.0CTAB–Al–Mt, the well resolved doublet of Si–O stretching vibration shifts from 1090 and 1032 to 1093 and 1037 cm^{-1}, respectively, and the band of Al–OH–Al bending vibration shifts from 917 to 914 cm^{-1}. This is coincident with that reported in the previous studies [13,14,33,34]. After the intercalation of hydroxy-Al, the band of Si(Al)–O stretching vibration shifts to higher frequency and the band of Si–O–Al stretching vibration shifts to lower one. This attributed to the interactions of the hydroxy-Al and surfactant cations within the montmorillonite interlayer space.

As shown in Fig. 6, the band at ca. 729 cm^{-1} is attributed to the Al–O stretching vibration (i.e. (M–O)$_{Td}$ stretching mode) in the hydroxy-Al (AlO$_4$Al$_{12}$ (OH)$_{24}$(H$_2$O)$_{12}$$^{7+}$) [35,36]. In this

Fig. 4. FTIR spectra of the CH$_2$ stretching bands of samples: (a) 0.2CTAB–Al–Mt; (b) 0.7CTAB–Al–Mt; (c) 2.0CTAB–Al–Mt; (d) 3.0CTAB–Al–Mt.
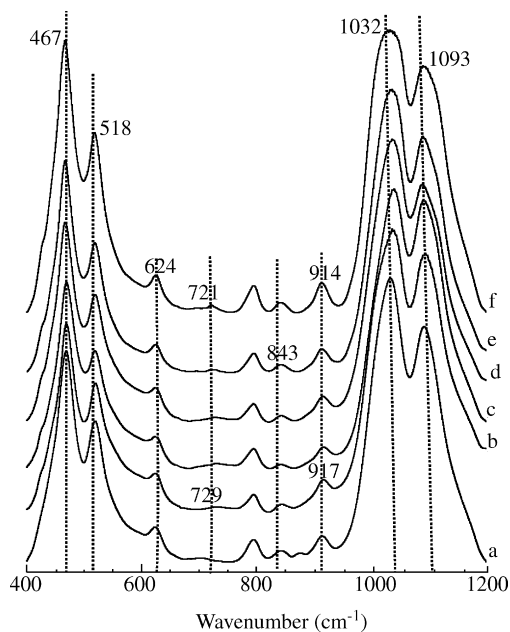

Fig. 5. FTIR spectra of samples in the range of 400–1200 cm^{-1}: (a) Na–Mt; (b) Al–Mt; (c) 0.2CTAB–Al–Mt; (d) 0.7CTAB–Al–Mt; (e) 2.0CTAB–Al–Mt; (f) 3.0CTAB–Al–Mt.

Table 2
Positions and assignments of the IR vibration bands observed in the range of 400–1200 cm^{-1}

Na–Mt	Al–Mt	0.2CTAB–Al–Mt	0.7CTAB–Al–Mt	2.0CTAB–Al–Mt	3.0CTAB–Al–Mt	Assignment
1092	1093	1092	1091	1090	1090	Si–O stretching
1033	1037	1037	1036	1035	1032	
915	917	917	916	914	914	Al–OH–Al
844	843	843	843	843	843	Si–O–Al, Al–OH–Mg
–	729	730	728	–	–	Keggin-(Al^{IV})OOH
–	–	–	–	721	721	CH$_2$– rocking
623	623	624	624	624	624	Si–O–Mg, Mg–OH
519	519	519	519	518	518	Si–O–Al (IV)
468	469	469	467	467	467	Si–O–Mg

study, this band appears in all the FTIR spectra of both Al–Mt and CTAB–Al–Mt complexes. Meanwhile, another absorption band at 721 cm^{-1} for the CH$_2$ rocking mode is observed in the spectra of CTAB–Al–Mt complexes (Fig. 6). This implies that both hydroxy-Al cations and CTAB have intercalated into the clay interlayer space. Furthermore, the relative intensities of the two bands strongly depend on the cation contents loaded in the complexes. For Al–Mt, a significant and broad band centered at 729 cm^{-1} is observed. However, with the increase of the loaded surfactant, the overlapping band, composed of the Al–O stretching vibration and CH$_2$ rocking mode, becomes well resolved, and the intensity of the CH$_2$ rocking mode increases obviously whereas that of Al–O stretching vibration decreases. This is in

accordance with the calculation of C/Si and Al/Si ratios as shown in Table 1. Our calculation demonstrates that, from Al–Mt to 3.0CTAB–Al–Mt, the C/Si ratio increases from 0 to 0.69 and the Al/Si ratio decreases from 0.50 to 0.25.

4. Conclusions

Inorganic–organic clay complexes are potential efficient sorbents to remove pollutants from water. Different from the previously reported route, in this study, CTAB–Al–montmorillonite complexes were synthesized by pre-modifying montmorillonite under different concentrations of surfactant, and then the organoclays were pillared with hydroxy-Al cations. The resultant inorganic–organic montmorillonite complexes were characterized using FTIR, with a combination of XRD, TG and chemical analysis. XRD patterns show that the basal spacings of the complexes strongly depends on the surfactant loadings in the corresponding organoclays used as the precursors, i.e. the complexes prepared from the organoclays with high surfactant loading display larger basal spacings than those prepared from the organoclays with low surfactant loading. Meanwhile, the content of the intercalated hydroxy-Al cations decreases with the increase of the loaded surfactants, resulted from the decrease of the mobility of the intercalated surfactants. With the intercalation of hydroxy-Al cations into clay interlayer space, part of the intercalated surfactants was removed and the conformation order of the surfactant decreases when compared with that of the corresponding organoclay. Both the bending vibration (ν_2) and stretching vibration (ν_1) of the sorbed water are sensitive to the clay surface property transformation from hydrophilicity to hydrophobicity. In other words, the frequency of the ν_2 mode shifts to higher frequency while the stretching vibration shifts to lower frequency, indicating that H$_2$O is less hydrogen bonded and the total sorbed water content decreases. The surface affinity (hydrophilicity and hydrophobicity) of the CTAB–Al–Mt complexes strongly depends on the surfactant loadings by pre-adsorption.

Further studies are under way to investigate the effects of the CTAB–Al–Mt complexes with different surfactant and hydroxy-Al cations contents on the sorption efficiency to various organic pollutants. Meanwhile, various spectroscopic techniques are being used to accurately determine the location of the sorbed organic pollutants in the complexes. This is of high importance for well understanding the sorption mechanism of
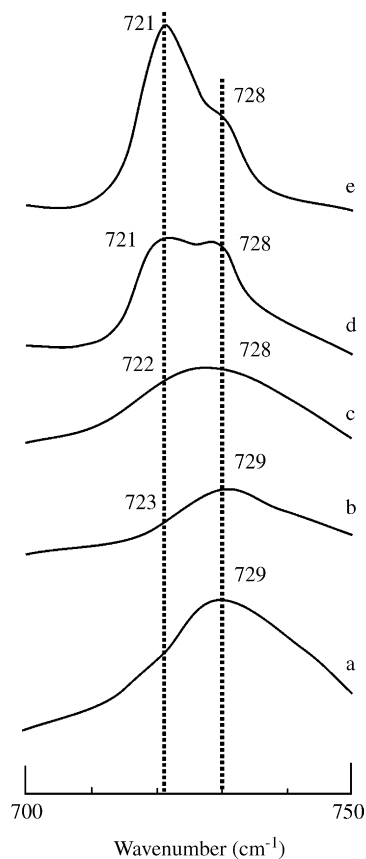

Fig. 6. FTIR spectra of samples in the range of 700–750 cm^{-1}: (a) Al–Mt; (b) 0.2CTAB–Al–Mt; (c) 0.7CTAB–Al–Mt; (d) 2.0CTAB–Al–Mt; (e) 3.0CTAB–Al–Mt.

inorganic–organic clay complexes to pollutants and the application in remediation of polluted environments.

References

[1] T.J. Pinnavaia, Science 220 (1983) 365.
[2] J.T. Kloprogge, J. Porous Mater. 5 (1998) 5.
[3] Z. Ding, J.T. Kloprogge, R.L. Frost, G.Q. Lu, H.Y. Zhu, J. Porous Mater. 8 (2001) 273.
[4] H.P. He, Z. Ding, J.X. Zhu, P. Yuan, Y.F. Xi, D. Yang, R.L. Frost, Clay Clay Miner. 53 (2005) 287.
[5] C.C. Wang, L.C. Juang, C.K. Lee, T.C. Hsu, J.F. Lee, H.P. Chao, J. Colloid Interface Sci. 280 (2004) 27.
[6] M. Cruz-Guzman, R. Celis, M.C. Hermosin, W.C. Koskinen, J. Cornejo, J. Agric. Food Chem. 53 (2005) 7502.
[7] M. Cruz-Guzman, R. Celis, M.C. Hermosin, J. Cornejo, Environ. Sci. Technol. 38 (2004) 180.
[8] H. Li, M. Eddaoudi, M. O'Keeffe, O.M. Yaghi, Nature 402 (1999) 276.
[9] K.R. Srinivasan, H.S. Fogler, Clay Clay Miner. 38 (1990) 277.
[10] P.X. Wu, Z.W. Liao, H.F. Zhang, J.C. Guo, Environ. Int. 26 (2001) 401.
[11] A. Elmchaouri, R. Mahboub, Colloid Surf. A: Physicochem. Eng. Aspect 259 (2005) 135.
[12] C.T. Johnston, G. Sposito, C. Erickson, Clay Clay Miner. 40 (1992) 722.
[13] J.T. Kloprogge, R.L. Frost, Appl. Clay Sci. 15 (1999) 431.
[14] S. Acemana, N. Lahav, S. Yariv, Thermochim. Acta 341 (1999) 349.
[15] J. Madejova, Vib. Spectrosc. 31 (2003) 1.
[16] H.P. He, F.L. Ray, J.X. Zhu, Spectroc. Acta A: Mol. Biomol. Spectrosc. 60 (2004) 2853.
[17] H.P. He, J.G. Guo, X.D. Xie, J.L. Peng, Environ. Int. 26 (2001) 347.
[18] J.X. Zhu, H.P. He, J.G. Guo, D. Yang, X.D. Xie, Chin. Sci. Bull. 48 (2003) 368.
[19] J.T. Kloprogge, R. Evans, L. Hickey, R.L. Frost, Appl. Clay Sci. 20 (2002) 157.
[20] P. Salerno, M.B. Asenjo, S. Mendioroz, Thermochim. Acta 379 (2001) 101.
[21] Q.H. Zeng, A.B. Yu, G.Q. Lu, R.K. Standish, J. Phys. Chem. B 108 (2004) 10025.
[22] H.P. He, J. Galy, J.F. Gerard, J. Phys. Chem. B 109 (2005) 13301.
[23] R.A. Vaia, R.K. Teukolsky, E.P. Giannelis, Chem. Mater. 6 (1994) 1017.
[24] W.Z. Xu, C.T. Johnston, P. Parker, S.F. Agnew, Clay Clay Miner. 48 (2000) 120.
[25] G.W. Brindley, R.E. Sempels, Clay Miner. 12 (1977) 229.
[26] J.Y. Bottero, J.M. Cases, F. Fiessinger, J.E. Poirier, J. Phys. Chem. 84 (1980) 2933.
[27] J. Madejova, M. Janek, P. Komadel, H.J. Herbert, H.C. Moog, Appl. Clay Sci. 20 (2002) 255.
[28] L.B. Yan, P.F. Low, C.B. Roth, Clay Clay Miner. 44 (1996) 749.
[29] L.B. Yan, C.B. Roth, P.F. Low, Langmuir 12 (1996) 4421.
[30] F.O. Libnau, O.M. Kvalheim, A.A. Christy, J. Toft, Vib. Spectrosc. 7 (1994) 243.
[31] N.V. Venkataraman, S. Vasudevan, J. Phys. Chem. B 105 (2001) 1805.
[32] Y.Q. Li, H. Ishida, Langmuir 19 (2003) 2479.
[33] J.T. Kloprogge, E. Booy, J.B.H. Jansen, J.W. Geus, Clay Miner. 29 (1994) 153.
[34] L.S. Li, X.S. Liu, Y. Ge, R. Xu, J. Rocha, J. Klinowski, J. Phys. Chem. 97 (1993) 10389.
[35] S.M. Bradley, R.A. Kydd, R.F. Howe, J. Colloid Interface Sci. 159 (1993) 405.
[36] S.M. Bradley, R.A. Kydd, C.A. Fyfe, Inorg. Chem. 31 (1992) 1181.